Mechanics of Solids
Vol. 40, No. 6, pp. 69–80, 2005

Izvestiya AN. MTT
No. 6, pp. 97–110, 2005

RHEOLOGICAL INSTABILITY AND LOCALIZATION OF STRAINS IN PLANE ELASTOPLASTIC SPECIMENS UNDER EXTENSION

V. N. Kukudzhanov and A. L. Levitin

(Received 12 May 2005)

We study buckling of plated specimens under extension for elastoplastic materials with various forms of stress-strain curves and plasticity conditions. Buckling of elastoplastic specimens in a supercritical state for material models taking into account damageability is accompanied by strain localization along shear bands and by necking. If damageability is not taken into account, then localization of extension prevails in specimens. We study the influence of the geometry of specimens and the physical properties of the material on the plastic strain localization process and on the character of fracture of specimens. It is shown that the factors determining the character of strain localization and of the subsequent fracture include, on the one hand, weakening and plastic compressibility of the material, which arise owing to the nucleation and growth of microdefects (primarily, microvoids), and, on the other hand, the geometric constraint condition on the plastic flow.

Our analysis enables a more realistic approach to the construction of medium models adequately describing experimental data on the falling section of the stress-strain curve as well as the character of strain localization and fracture of specimens under extension.

1. INTRODUCTION

Numerical modeling of buckling problems is one of the most complicated challenges in continuum mechanics. Finding critical parameter values at which buckling occurs is a problem of ordinary complexity. But the problem of determining the behavior of the system beyond the ultimate load (i.e., describing how the process develops in a supercritical state and finding the mechanism and specific features of its development) is incomparably more complicated owing to instability and ambiguity. This problem can be solved if the post-buckling process does not have the character of random motion and if, despite the obvious ambiguity and the dependence of the solution on the discretization of the problem (sizes and shapes of partition elements, the numerical method used, and other random factors), one can single out regular component of the structure. The issue is to distinguish casual from natural. The problem cannot be solved analytically, and it is not easy to solve it numerically, since, as a rule, there is no rigorous mathematical proof of the reliability and/or stability of the numerical method itself. Hence one cannot be sure that physical instability is not combined with purely numerical effects. To understand the mechanism of the phenomenon, one needs to carry out a vast amount of computations for various values of the problem parameters and closely analyze the results.

The study of a supercritical state is not only important from the viewpoint of fundamental science but also has a purely applied merit in many cases, say, when determining the bearing strength of statically indeterminate rod systems. The clear understanding of causes of and conditions for plastic strain localization in shear bands is very important in describing extension fracture in many technological processes (stretch forming, drawing, and rolling).

Buckling of a specimen under extension and its supercritical behavior precede fracture. Without examining these processes, one cannot understand and explain the fracture process. This problem is one of the most important problems of modern mechanics of deformable solids and draws the attention of numerous researchers [1–8].

When studying buckling of materials, one should first clarify buckling criteria. In mechanics of deformable solids, these problems have been studied rather comprehensively for classical medium models (elastic and elastoplastic) [2, 9–11]. However, the supply of models has increased dramatically in the last decades, mainly owing to models

related to brittle and ductile fracture and to the study of the influence of damage. Buckling is poorly studied for such media yet [12, 13].

When studying the stability of materials in damaged state (i.e. close to fracture), one should, in contrast to the case of a classical elastoplastic medium (satisfying the von Mises plasticity condition) take into account the plastic compressibility of the material, which is a consequence of void nucleation. This results in an essential modification of the plasticity condition [1–4].

Buckling of flat specimens under extension is followed by the plastic strain localization, necking, and eventually the fracture of the specimen. We consider various material models for which the Drucker stability condition is violated: 1) a perfectly plastic model; 2) a model with initial plastic hardening and with exit of the material stress-strain curve to ideal plasticity under a plasticity condition of the von Mises type; 3) a model of a porous material with the same stress-strain curves for the matrix material under the Garson plasticity condition for the effective material (the GTN-model [1]).

We show that, under the von Mises plasticity condition, necking occurs only in the case of a perfectly plastic or falling material stress-strain curve. It follows that the "true" stress-strain curve usually obtained in standard extension experiments, which does not have a weakening section, cannot be accepted as the material stress-strain curve included in the material constitutive equations.

All three considered models result in the bifurcation instability of the extension process. In the supercritical state, to single out a certain branch of the solution, a perturbation was introduced in the form of a small notch in the central part of an specimen. For the above-mentioned models, the mechanisms of evolution of shear and extension localization bands are studied, and differences in their nucleation are revealed.

For the model of plastic flow under the von Mises plasticity condition, the neck is formed in the specimen owing not to shear but to the extension localization and to transverse thinning in a neighborhood of the cross-section where the extension is localized. Accordingly, fracture in these models occurs by separation along the plane normal to the extension direction.

Necking and tensile failure under plane strain conditions in the GTN-model taking into account void nucleation occur owing to shear localization (instead of separation, as in the case of von Mises extension). It is shown that the most adequate pattern of formation and evolution of shear localization bands is given by the model taking into account microvoid nucleation and growth.

2. MODELS OF MATERIALS

2.1. Elastoplastic material. We consider the model of an elastoplastic material based on the following hypotheses of the theory of plastic flow [14, 15].

• Additivity of elastic and plastic strains,

$$\varepsilon = \varepsilon^e + \varepsilon^p. \tag{1}$$

• The plasticity condition in the general case of an isotropic body, depending on invariants of the stress tensor S_i, the plastic strain rate tensor $\dot{I}_i^p$, and interior parameters χ_k,

$$F(S_i, \dot{I}_i^p, \chi_k) = 0. \tag{2}$$

In the case of a perfectly plastic material, the plasticity condition is simplified dramatically and acquires the form

$$F = \frac{F}{\sigma_Y} - 1 = 0, \tag{3}$$

where $S = (s_{ij}s_{ij})^{1/2}$ is the strain intensity and σ_Y is the yield strength of the material.

• The associated plastic flow law,

$$\dot{\varepsilon}_{ij}^p = \dot{\lambda}\frac{\partial F}{\partial \sigma_{ij}}. \tag{4}$$

• Evolution equations for the interior variables. In our case, this is an equation for the material hardening parameter χ and the damage f.

2.2. Damageable elastoplastic material with voids. The GTN-model. Experiments show that numerous voids growing with the plastic strain are formed in a prefractured material. Hence the material becomes highly compressible; this fact cannot be neglected and is taken into account in the model of an elastoplastic porous material.

Modeling of necking and the subsequent fracture is based on the equations for an elastoplastic porous material suggested by Gurson [1] and further developed by Tvergaard and Needleman [2, 3]. In the literature, this model is known as the GTN-model. It takes into account the onset and growth of voids only under extension. The GTN-model is a generalization of the classical theory of flow under the von Mises plasticity condition and takes into account the influence of plastic compressibility of the material owing to void formation in the prefracture state.

The GTN-model considers an effective porous material with an elastoplastic matrix. The yield function for the effective material has the form

$$F = \left(\frac{S}{\sigma_Y}\right)^2 + 2q_1 f \cosh\left(\frac{3q_2\sigma_{kk}}{2\sigma_Y}\right) - (1 + q_1^2 f^2) = 0, \tag{5}$$

where q_1 and q_2 are adjustable parameters introduced by Tvergaard and Needleman [3], $S = \left(\frac{3}{2}s_{ij}s_{ij}\right)^{1/2}$ is the stress intensity in the effective material, $\sigma_{kk} = -p$ is the first invariant of the stress tensor (pressure), $s_{ij} = \sigma_{ij} - \frac{1}{3}\sigma_{kk}\delta_{ij}$ is the stress deviator, σ_Y is the yield strength of the material, and σ_{ij} is the Cauchy stress tensor.

The damageability structure parameter is porosity $f = V_{\text{por}}/V$, equal to the ratio of volume of the fractured material (voids) to the total volume of the material.

In condition (1), along with porosity f, the ratio σ_{kk}/σ_Y has a very strong influence. The yield strength σ_Y is defined from the equality of work for the plastic matrix and the effective material:

$$(1 - f)\sigma_Y\dot{\bar{\varepsilon}}^p_m = \sigma_{ij}\dot{\varepsilon}^p_{ij}, \tag{6}$$

where $\bar{\varepsilon}^p_m$ is the plastic strain rate intensity in the matrix.

For a hardened elastoplastic material, the relationship between $\bar{\varepsilon}^p_m$ and σ_Y is given by Eq. (2) in the form

$$\dot{\bar{\varepsilon}}^p_m = \left(\frac{1}{E_T} - \frac{1}{E}\right)\dot{\sigma}_Y,$$

where the instantaneous elastic modulus $E_T(\sigma_Y)$ is determined from the uniaxial extension stress-strain curve of the material.

The evolution equation for porosity consists of two terms,

$$\dot{f} = \dot{f}_{\text{gr}} + \dot{f}_{\text{nucl}}, \tag{7}$$

where the first term $\dot{f}_{\text{gr}}$ describes the growth of existing voids and the second term $\dot{f}_{\text{nucl}}$ describes the formation of new voids. The void growth is related to the volume plastic strain ε^p_{kk} and is determined by the mass conservation law,

$$\dot{f}_{\text{gr}} = (1 - f)\dot{\varepsilon}^p_{kk}. \tag{8}$$

The onset of new voids is specified by the relation

$$\dot{f}_{\text{nucl}} = A\dot{\bar{\varepsilon}}^p_m. \tag{9}$$

Here $\bar{\varepsilon}^p_m$ is the plastic strain intensity in the matrix. The relation

$$A = \frac{f_N}{s_N\sqrt{2\pi}}\exp\left[-\frac{1}{2}\left(\frac{\bar{\varepsilon}^p_m - \varepsilon_N}{s_N}\right)^2\right] \tag{10}$$

for the coefficient A is defined as the normal distribution of strains $\bar{\varepsilon}^p_m$ with mean value ε_N and standard deviation s_N, and f_N is the volume fraction of the incipient voids. The voids form only under extension.

The classical elastoplastic models based on the von Mises plasticity condition do not take into account the influence of the first invariant of the stress tensor (pressure) on the plastic properties of the material.

In the special case $f = 0$, the plasticity condition (1) passes into the von Mises plasticity condition, where σ_Y can be assumed to depend on a hardening parameter, for example, on the Odquist parameter

$$\chi = \int_0^t \sqrt{\dot{\varepsilon}^p_{ij}\dot{\varepsilon}^p_{ij}}\,dt$$

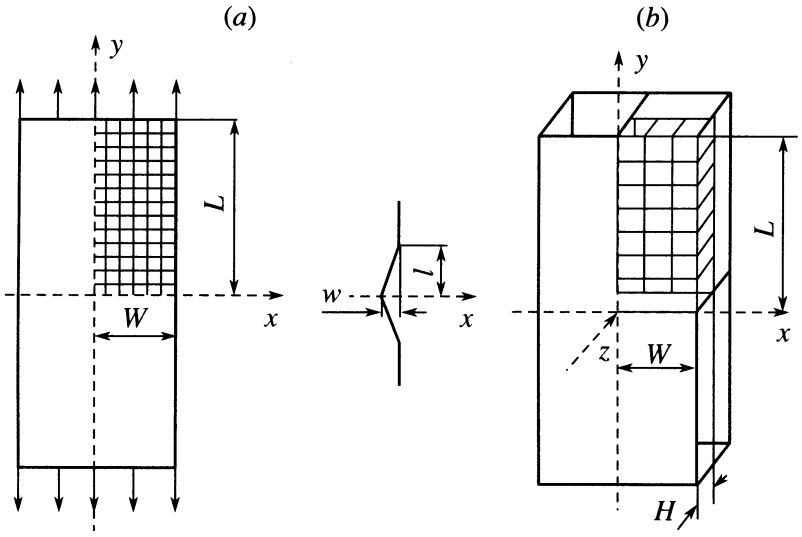

Fig. 1

or the plastic work

$$W^p = \int_0^{\varepsilon_{ij}^p} \sigma_{ij}\, d\varepsilon_{ij}^p.$$

2.3. Fracture criteria for a material. To study fracture, one should supplement the GTN-model with fracture criteria.

Fracture criteria are to some extent related to the very statement of the model. For example, plasticity is related to shear strain if the plastic incompressibility of the material is assumed. (The spherical part of the stress tensor, pressure, (almost) does not contribute to strain, and the elastic component is small.) It is natural to assume that such a material can fail only after the shear strain reaches some limit,

$$\chi = \int_0^t \sqrt{\dot{\varepsilon}_{ij}^p \dot{\varepsilon}_{ij}^p}\, dt \le \chi_{\text{cr}}. \tag{11}$$

If the material is strongly compressible, then fracture is determined by critical porosity,

$$f \le f_{\text{cr}}. \tag{12}$$

Thus, when studying fracture of a damaged elastoplastic material, one should verify two independent conditions, namely, the shear strain intensity (11) and the porosity (12). Fracture happens according to the criterion whose is satisfied earlier.

3. STATEMENT OF THE PROBLEM AND THE SOLUTION METHOD

We consider quasi-static extension of continuous homogeneous specimens made of a nonlinear material and weakened by a small outer notch. The computations were carried out for flat rectangular specimens (Fig. 1). A uniform displacement increasing in time at a constant rate was applied to the end faces of the specimen. For the second condition at the end face, we take the condition of absence of shearing stresses. These conditions ensure the exact solution in the form of homogeneous uniaxial extension along the length of the specimen; this case is easiest for the computation of buckling. Should, for example, the second condition be that the transverse displacement is zero, this would violate the homogeneity of the stress-strain state near the end face. We study the stability of this solution and supercritical modes of behavior of the specimen until complete fracture. Buckling manifests itself as a deviation from the homogeneous state caused by small perturbations.

The elastic characteristics of the material were $E = 300$ MPa and $\nu = 0.3$. The dependence of the yield strength σ_Y of the plastic material of the matrix on the strain is given in Fig. 2. In some computations, an elastic–perfectly plastic material was considered (curve 1) with yield strength $\sigma_Y \equiv \sigma_Y^0 = 1.00$ MPa and $\varepsilon_Y^0 \approx 3.34 \cdot 10^{-2}$. In other computations,

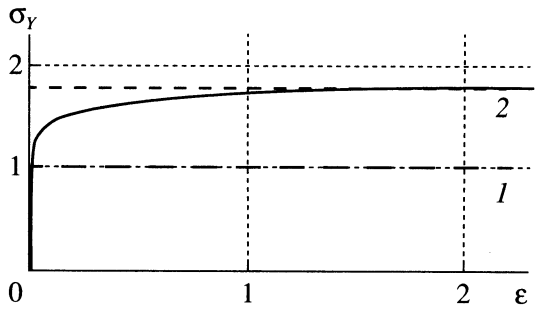

Fig. 2

a curve with an initial plastic hardening part was used (curve 2): plasticity starts at $\sigma_Y^0 = 1.00$, and the curve approaches perfect plasticity at $\sigma_Y^* = 1.795$ and $\varepsilon_Y^* \approx 1.73$.

The parameters characterizing the GTN-model were taken as follows: $\rho_0 = 0.0$, $q_1 = 1.5$, $q_2 = 1.0$, $\varepsilon_N = 0.3$, $s_N = 0.1$, and $f_N = 0.1$.

The initial dimensions of the specimen were the same in all computations (Fig. 1); the rod had half-height $L = 4$ mm, half-width $W = 1$ mm, notch half-height $l = 0.030$ mm, and notch depth $w = 0.005$ mm. The half-thickness of the specimen (when modeling thin plates) was $H = 0.05$ mm or $H = 0.10$ mm.

In space, a finite-element approximation on a Lagrangian mesh was used, which permits one to keep track of the deformation of the elements visually. By virtue of symmetry, the domain to be modeled is one-fourth of the specimen (Fig. 1); it is divided by the mesh into quadrangular elements (a two-dimensional plane strain problem; $\varepsilon_z = 0$) or cubic elements (a spatial problem). The extension of plated specimens was modeled with the use of four-point bilinear quadrangular finite elements. Symmetry conditions ($u_n = 0$ and $\sigma_{xy} = 0$) were posed on the left and lower sides of the region. The right side is stress free. A vertical displacement increasing at a constant rate was given on the upper boundary.

To avoid introducing numerical inhomogeneity, which can distort the solution of the problem at the transition to a supercritical state, the specimen was uniformly divided into rectangular finite elements along the entire domain. The height of an element did not exceed the height l of a small notch placed on the exterior side at the center of the specimen (Fig. 1,*a*). Finite-element meshes of 20×133 and 40×160 elements in the first and second layers, respectively, of the notch band were used in the computations. In the former case the horizontal dimension of an element was greater than the vertical dimension, so that the elements would approach the square shape under strain. In the second case, the elements were square-shaped outside the notch.

The extension of thin plated specimens was modeled in the spatial statement of the problem, since the transverse thinning in the localization region is essential in this case (Fig. 1,*b*). Eight-point linear cubic elements were used. Symmetry conditions were posed on the planes $x = 0$, $y = 0$, and $z = 0$. On the upper side, the vertical displacement u_y was specified. Two thin specimens with various half-thickness $H = 0.05$ mm and $H = 0.10$ mm ere considered, one or two elements were arranged in the z-direction, and the finite-element mesh used in the computations comprised $20 \times 80 \times 1$ and $20 \times 80 \times 2$ elements, respectively.

In all considered problems, a finite-element approximation on a Lagrangian mesh with respect to space and a finite-difference approximation with respect to time were used.

The constitutive equations of the material are substantially nonlinear, and the successive loading method with Newton–Raphson iterations at each variable time step [16] was applied to obtain the solution. Note that the rod upper end face displacement is proportional to the time step and the strain rate of the specimen is constant, $v = 0.5$ mm/sec. The maximum admissible step $\Delta t_{\max}$ in conventional time was chosen from the condition that the strain increment $\Delta\varepsilon$ of the overall specimen should not exceed the maximum elastic strain $\varepsilon_Y = \sigma_Y^0 / E$ at any step.

4. NECKING AND BUCKLING UNDER PLANE STRAIN

First, we consider necking mechanisms for a plated specimen under various plasticity conditions and various stress-strain curves of the material. We reveal the effect of the notch on the stress-strain state and buckling and study the mechanism responsible for the onset of localization bands and fracture of the specimens. A majority of computations presented in this section were carried out on a mesh of 20×133 elements with the maximum admissible quasi-time step $\Delta t_{\max} = 0.0125$ sec. The initial configuration of the specimen is shown by an open frame; the current configuration is shown by the deformed mesh.

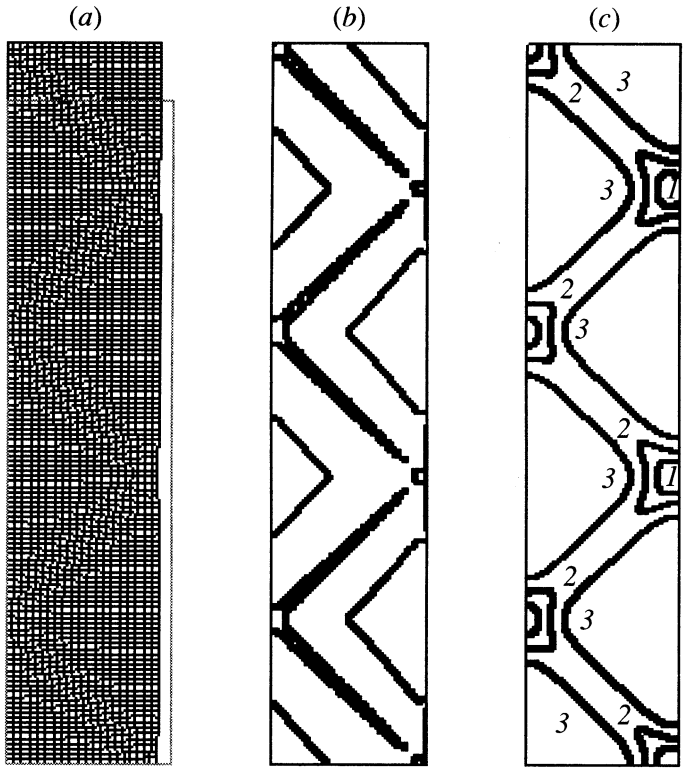

Fig. 3

4.1. A homogeneous perfectly plastic specimen. For the extension of a specimen made of a perfectly plastic material, the Drucker condition is simultaneously violated in the entire specimen. Buckling has a bifurcation character. A very certain periodic structure of localization centers is formed, which corresponds at the initial stage to the rigid-plastic solution of the problem [14] (Fig. 3) and is determined by the geometric size ratio of the specimen. For u = 0.35 mm and ε = 8.75%, Fig. 3 shows the deformation of the Lagrangian mesh (Fig. 3,*a*), the stress intensity isolines S = 1.001 MPa (Fig. 3,*b*), and the plastic strain intensity isolines I_1^p = 0.0263, I_2^p = 0.0185, and I_3^p = 0.0108 (Fig. 3,*c*).

The supercritical strain occurs similarly to linear stability problems, where the solution modes differ from each other in the number of harmonics. Likewise, in nonlinear rheological instability problems the solutions differ in the number of necks being formed. There arise a number of localization centers along the rod, each of which can potentially form a neck. But this periodic structure is unstable and collapses owing to random perturbations (numerical errors and/or geometric irregularities). With increasing strain, the localization at one or two centers proves to be larger than at the other centers. They take all subsequent strain. As a result, the strain is frozen in the other necks and rapidly grows in one of the necks, which results in fracture. For u = 0.75 mm and ε = 18.75%, Fig. 4 shows the deformation of the Lagrangian mesh (Fig. 4,*a*) and the plastic strain intensity isolines I_1^p = 1.01 and I_2^p = 0.543 (Fig. 4,*b*). We see that in the final state there are two necks at the ends of the specimen (the effect of inhomogeneity due to boundary conditions). It is typical that they are close to each other in shape and stress-strain state. This proves that each of the localization centers develops according to the same law, which is completely determined rather than chaotic.

To obtain the least mode corresponding to one neck, one should create a small perturbation sufficient for suppressing the other random perturbations in the specimen.

Another stabilizing factor is the initial plastic hardening, always present in real materials, which was taken into account with the use of curve 2 in Fig. 2.

The stress-strain state in a material is homogeneous until buckling. If the material is hardened in the entire strain range, no buckling is observed even under artificial perturbations. A local violation of Drucker's postulate is necessary for buckling; i.e., the material stress-strain curve should be bounded and enter ideal plasticity or loss of strength (Fig. 2).

4.2. The extension of a notched specimen. A von Mises material with initial plastic hardening. The notch is a stress raiser; therefore, the maximum stress occurs in the specimen section containing the small notch.

Figure 5 shows the stress intensity isolines S at three initial stages of extension (prior to buckling). Figure 5,

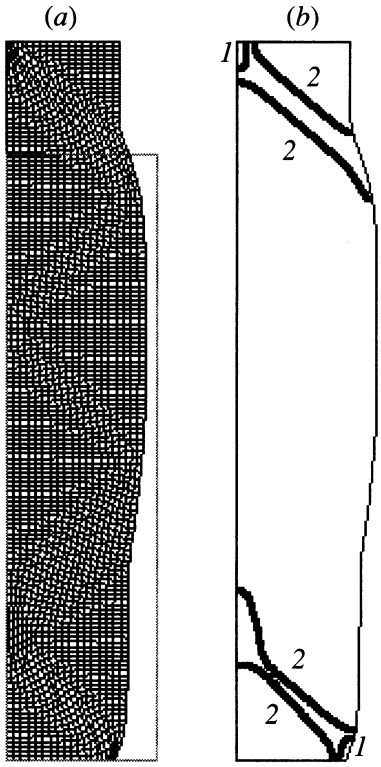

Fig. 4

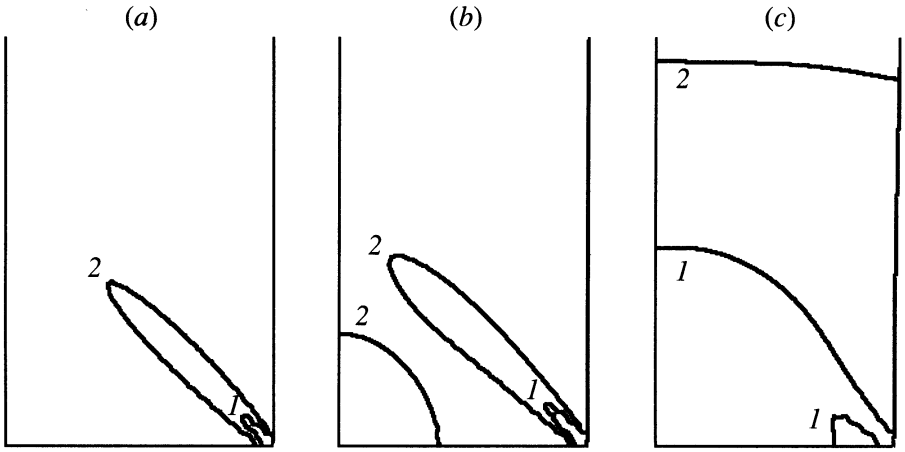

Fig. 5

a corresponds to u = 0.20 mm, ε = 5%, S_1 = 1.345 MPa, S_2 = 1.339 MPa. Figure 5,*b* corresponds to u = 0.49 mm, ε = 12.25%, S_1 = 1.476 MPa, S_2 = 1.472 MPa. Figure 5,*c* corresponds to u = 0.56 mm, ε = 14.00%, S_1 = 1.516 MPa, S_2 = 1.499 MPa. There is a band, issuing at an angle about 45° from the notch, in which the stress intensity is first approximately 0.5–2% larger than in the remaining part of the specimen (Fig. 5,*a*). Outside the band, the stressed state of the specimen is almost homogeneous (the spread coincides with the computational error). In the immediate vicinity of the notch, on each side of the band there are mini-regions of unloaded material. (The stresses there are approximately 1% less than in the remaining part of the specimen.) This is valid both for the elastic and for the hardening plastic condition.

After the stress intensity in the band (up to the vertical symmetry axis) exceeds $\frac{2}{3}\sigma_Y^* \approx 1.466$ MPa, a region of increased stresses begins to form at the center of the specimen at the intersection of symmetry axes (Fig. 5,*b*).

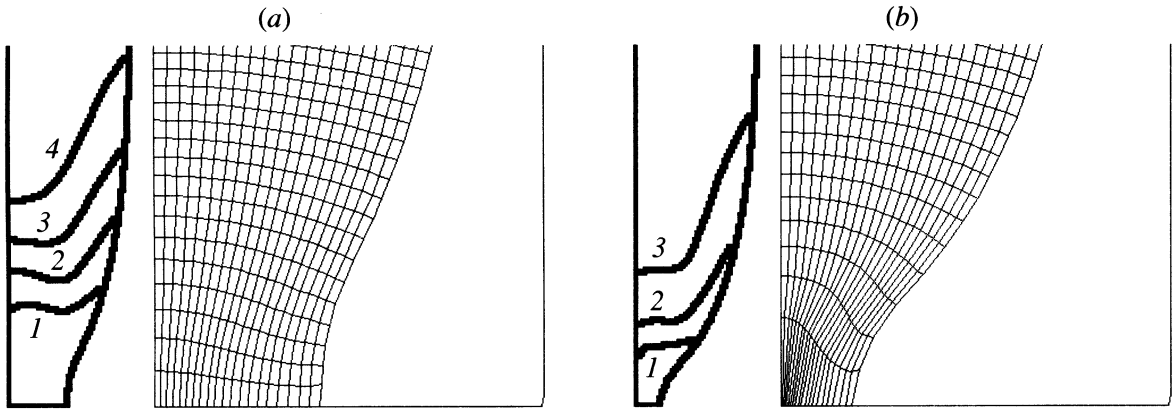

Fig. 6

Increasing, the new region merges with the shear band. The stress intensity at the center of the specimen becomes larger than that near the small notch. The subsequent stress intensity growth occurs not from the notch but from the center of the specimen, the increased stress intensity region occupies the entire cross-section of the specimen, and necking begins (Fig. 5,*c*). Note that necking begins much earlier in the specimen with a notch than in a homogeneous specimen.

Figure 6 shows the finite-element mesh during the specimen deformation process. We see that only one neck is formed at the rod center, where the small notch was located. This is explained by the fact that in the presence of hardening the critical stress occurs not in all cross-sections simultaneously (as is the case for a perfectly plastic material) but only in one weakened cross-section. In a neighborhood of the neck, there is mixed shear-extension strain. There is no pronounced shear band and no sharp localization of shear strain. The neck mainly develops by elongating in the central cross-section. The fracture occurs by separation. For u = 0.95 mm and ε = 23.75% (Fig. 6,*a*, the stress intensity isolines S_1 = 1.650 MPa, S_2 = 1.487 MPa, S_3 = 1.325 MPa, and S_4 = 1.162 MPa), the extension strain in the central cross-section is of the same order as nearby, but for u = 1.10 mm and ε = 27.50% (Fig. 6,*b*, the stress intensity isolines S_1 = 1.776 MPa, S_2 = 1.134 MPa, and S_3 = 0.813 MPa) the extension strain in the central cross-section is several times larger than nearby and makes 250–300%; i.e. one has localization of extension strains. The maximum strain intensity is attained in the central cross-section on the rod axis (rather than near the notch), from which the crack begins to propagate. We see that for a larger elongation (Fig. 6,*b*) unloading occurs near the neck (between isolines 1–3) and the plastic strain is frozen.

4.3. A GTN-material with initial plastic hardening. The extension of a homogeneous specimen. For a GTN-material, the stress-strain state is affected by the first invariant of stresses σ_{kk}, and the form of the stress-strain state is characterized by the ratio σ_{kk}/σ_Y, where σ_Y is the yield strength of the effective material.

The supercritical strain process in a homogeneous specimen develops at the initial stage qualitatively by the same scheme as in a perfectly plastic material without damage. First, there occurs a periodic unstable system of necks. Localization happens much earlier than in the classical model, since taking into account porosity in the GTN-model results in a sharp weakening of the material in the localization region. With increasing strain, localization in one of structure elements proves to be larger, and the periodic system collapses. But at a later stage, when porosity becomes noticeable, the stress-strain pattern changes dramatically, and the solution structure is very different from that without taking into account damageability.

4.4. A GTN-material with initial plastic hardening. The extension of a notched specimen. The initial state is similar to that in the classical model (Fig. 5). With increasing elongation of the specimen, voids onset and grow in the material, which results in weakening of the material and a sharper localization than in the classical model. The notch concentrates stresses, the strain is stably (with respect to numerical perturbations in the computations) localized near, and a neck is formed.

Consider the stage in which localization is not large, the neck only originates, but porosity is already essential. Then the stress-strain state in a GTN-material differs from the stress-strain state in a classical elastoplastic material (compare Fig. 7 with Fig. 5,*c* and Fig. 6). This is the effect of the first invariant of stresses and of the damage. For u = 0.60 mm and ε = 15.00%, Fig. 7 shows the deformation of a finite-element mesh (Fig. 7,*a*), the plastic strain intensity isolines I_1^p = 0.292, I_2^p = 0.235, and I_3^p = 0.178 (Fig. 7,*b*), and the porosity isolines f_1 = 3.0%, f_2 = 2.3%, f_3 = 1.6%, and f_4 = 0.9% (Fig. 7,*c*). For u = 0.75 mm and ε = 18.75%, Fig. 8 shows the deformation of a finite-element

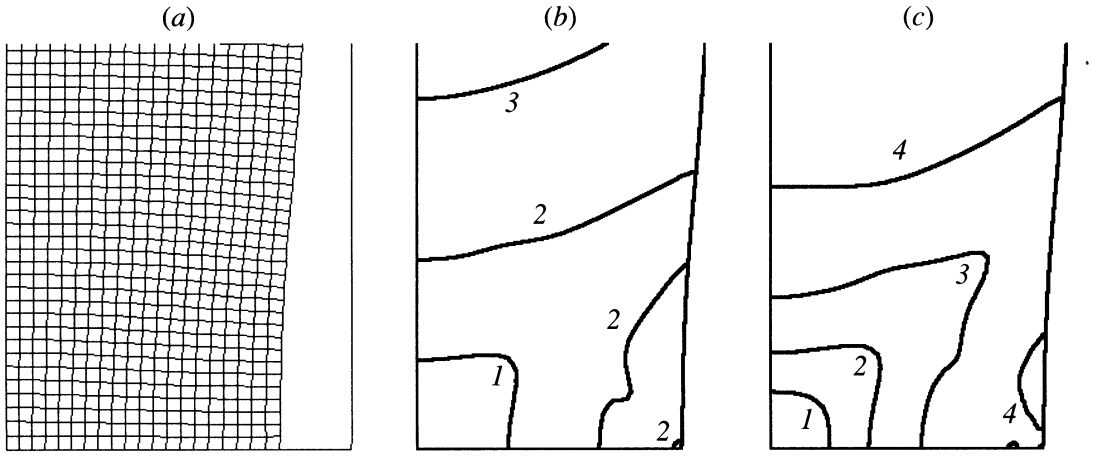

Fig. 7

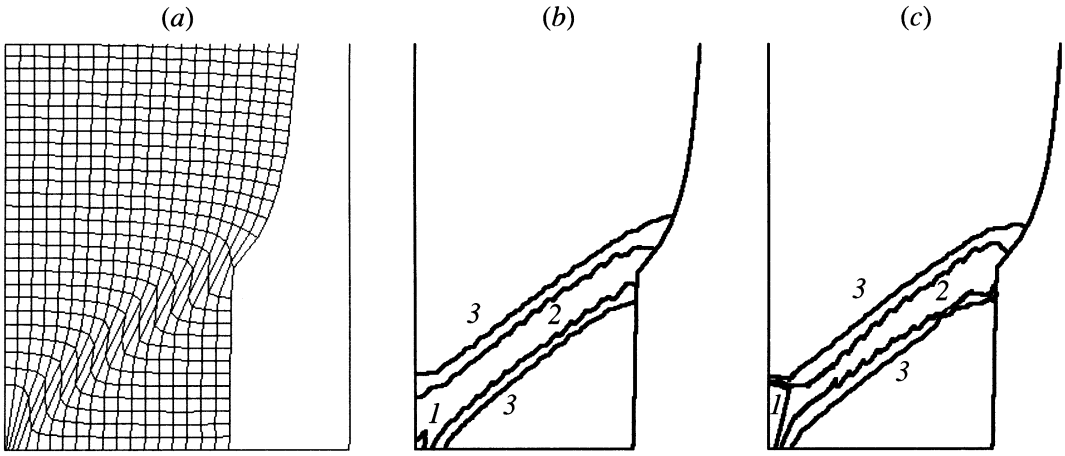

Fig. 8

mesh (Fig. 8,*a*), the plastic strain intensity isolines I_1^p = 1.564, I_2^p = 1.083, and I_3^p = 0.602 (Fig. 8,*b*), and the porosity isolines f_1 = 55%, f_2 = 28%, and f_3 = 14% (Fig. 8,*c*).

With increasing extension of the specimen, the uniform extension region grows and is localized, and the solutions differ qualitatively. This is seen from the comparison of Figs. 6 and 7 with Fig. 4,*b*.

The region of increased stress intensity S, uniform extension σ_{kk}, and porosity f is localized at the center of the specimen (at the intersection of symmetry axes). With increasing extension, there is a sharp increase in strains and porosity, localized in a narrow band issuing from the center of the specimen at an angle about 45°. The material outside the localization band is unloaded. The elements in the localization band take practically all strain, and a "plastic wedge" (part of the material drawn into the specimen almost without deformation) is formed on the horizontal symmetry axis.

4.5. Comparison of the supercritical deformation results for models with and without damageability. Integral diagrams. Figure 9 gives the conventional and true stress-strain curves constructed for notched specimens made of an elastoplastic material with initial hardening (Fig. 9,*a*) and a GTN-material with initial plastic hardening of the matrix (Fig. 9,*b*). None of them coincides with the material stress-strain curve used in the computations.

The model for which the stress-strain curve of the material (matrix) includes initial hardening (Fig. 2) is much more stable than the perfectly plastic model. Changes in the computation parameters (the integration step $\Delta t_{\max}$ with respect to conventional "time" and the mesh size) have practically no effect on the results of computations (Fig. 9).

The specific buckling mode (the number and location of necks and localization bands) for a perfectly plastic specimen (Fig. 9) substantially depends on the computation parameters (the finite-element mesh size and the limit integration step $\Delta t_{\max}$ with respect to loading). The introduction of even a small notch for a model with initial plastic

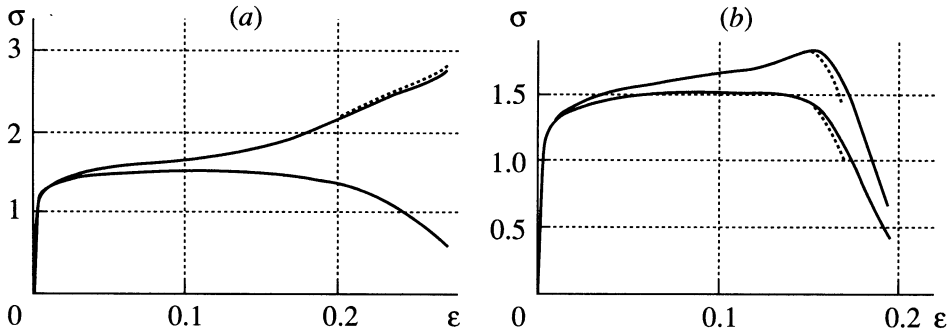

Fig. 9

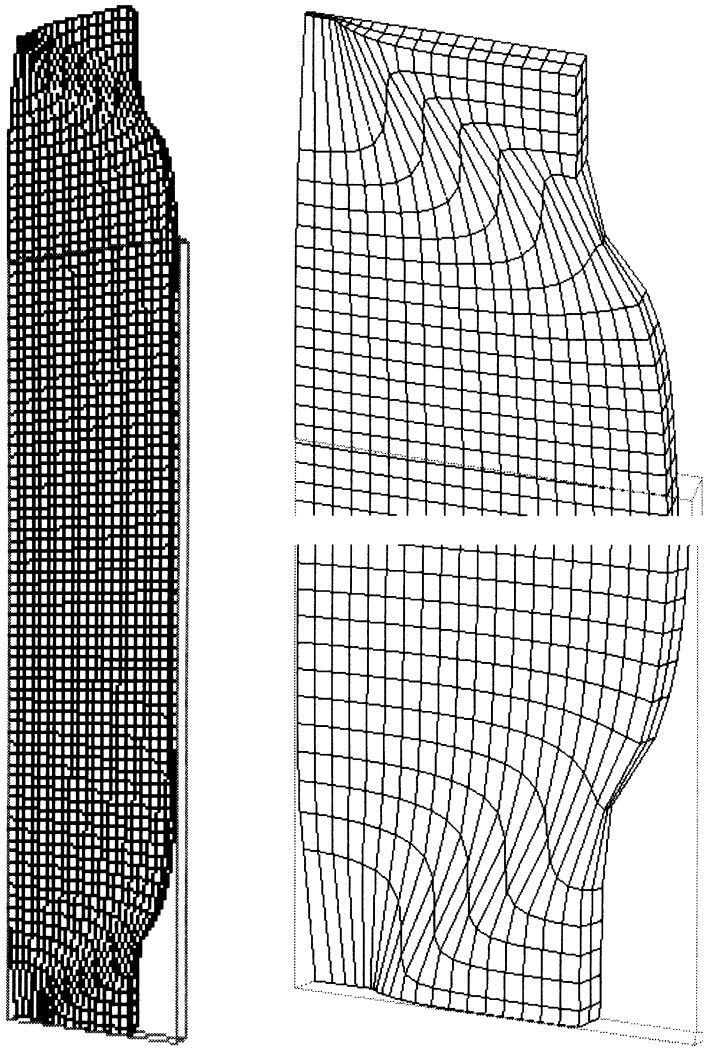

Fig. 10

hardening results in a perturbation sufficient to cause buckling and strain localization near the notch.

Practically, the integral true and conventional stress-strain diagrams differ only after the transition into a supercritical state. For notched specimens with initial plastic hardening, the integral stress-strain diagrams very weakly depend on the computation parameters (the finite-element mesh size and the limit integration step $\Delta t_{\max}$ with respect to loading) and change only slightly under changes in the problem discretization parameters.

5. NECKING IN THIN NOTCHED PLATES

To take into account transverse thinning in a thin plate, three-dimensional spatial modeling is needed. We shall give the results obtained for the damageable material (the GTN-model) with initial plastic hardening of the matrix and with a small notch in the specimen.

Here the effects of the notch proves to be insufficient for suppressing the nonphysical numerical perturbations, and two necks are observed in Fig. 10. Their formation is favored by the inexact realization of the natural boundary condition, which is satisfied only in the weak sense in the finite-element method.

In thin plates, transverse thinning in the direction of the z-axis in the localization band is essential. Just as for a thick plate (Fig. 5) the stress intensity at the initial stage grows in the direction from the notch to the vertical symmetry plane of the specimen and then occupies the domain at the center of the specimen at the intersection of the horizontal and vertical symmetry axes. Localization develops as a combination of shear and separation. In the localization band, a sharp lateral contraction almost up to zero thickness is observed. The formation and motion of a "plastic wedge" to the vertical axis is clearly visible. (It is this process that creates the neck.) In contrast to a thick plate, the localization band in a thin plate passes at a smaller angle about $35^\circ - 40^\circ$, which is close to the rigid-plastic solution for a plan stress state [9, 14]. The localization band does not issue directly from the center of the specimen but is a little shifted to the edge. There is a uniform extension and fracture region developing in a neighborhood of the center; as a result, an opening mode crack is formed here. Closer to the edge, the crack passes into shear fracture at an angle to the specimen axis. The larger the ratio of the plate thickness H to its width W, the stronger this effect.

Figure 10 shows the pattern of formation of shear bands and thinning of the plate in the direction of the z-axis. Note that the solution almost completely reproduces itself in two distinct top and bottom necks, even though the conditions in discrete form on the upper and lower sides of an specimen are different. This is evidence of the stable character of the solution within one neck structure element and confirms the bifurcation character of rheological buckling of elastoplastic specimens.

6. CONCLUSIONS

The neck is formed only if the Drucker material ($\Delta\sigma\Delta\varepsilon > 0$) stability criterion is violated, i.e., if the material stress-strain curve ends with a decreasing or horizontal section.

Rheological buckling has a bifurcation character, which consists in the formation of an unstable periodic system of structure localization elements (modes) in the supercritical stage. At the same time, the solution within each mode (neck) is not very sensitive to perturbations.

An Initial perturbation permits one to single out one of the branches of the solution. The perturbation should be stronger than the other perturbations related to inhomogeneities in the computation process (numerical errors, boundary conditions, etc.).

If void formation is taken into account, then the plasticity condition is strongly affected by the first invariant σ_{kk} of the stress tensor and the plastic compressibility of the material, which have a substantial influence on the strain localization and the formation of shear bands. The introduction of softening $\sigma_Y(f)$ alone would not be sufficient for obtaining a pronounced shear localization; one has to consider the influence of the uniform extension σ_{kk}.

Taking into account damage under plane strain conditions results in a clear localization of strains in the form of a shear band. The fracture of the specimen occurs along localized shear bands, unlike the fracture of a specimen under the von Mises plasticity condition, which occurs by separation.

In a thin plated specimen (a plane stress state) of a damageable elastoplastic material, the shear band is formed at an angle of $35^\circ - 40^\circ$ to the horizontal axis. As the thickness of the specimen increases, a uniform extension band is formed near its center, and the shear band is displaced to the exterior surface, which results in fracture by separation along a plane surface near the axis and along a tilted shear surface closer to the lateral surface of the specimen. The thinning of the specimen happens in two directions, Ox and Oz.

The comparison of modeling results with experimental data shows that the model of a porous medium describes the fracture of an elastoplastic material quite adequately.

ACKNOWLEDGMENTS

The research was carried out under support of the Russian Foundation for Basic Research (grant No. 03-01-00701) and the Program of Basic Research of the Russian Academy of Sciences (Department of Energetics, Mechanical Engineering, Mechanics and Control Processes of the Russian Academy of Sciences, Project No. 14).

REFERENCES

[1] A. L. Gurson, “Continuum Theory of Ductile Rupture by Void Nucleation and Growth: Part I. Yield Criteria and Flow Rules for Porous Ductile Materials,” J. Engin. Mater, and Techn., Vol. 99, pp. 2–15, 1977.
[2] V. Tvergaard, “Influence of Voids on Shear Band Instabilities under Plane Strain Condition,” Intern. J. Fracture Mechanics, Vol. 17, pp. 389–407, 1981.
[3] A. Needleman and V. Tvergaard, Material Strain-Rate Sensitivity in the Round Tensile Bar, Brown University Report, Division of Engineering, 1985.
[4] V. N. Kukudzhanov, “Micromechanical model of fracture of an inelastic material and its application to the investigation of strain localization,” Izv. RAN. MTT [Mechanics of Solids], No. 5, pp. 72–87, 1999.
[5] V. G. Bazhenov, A. N. Kibets, P. V. Laptev, and S. L. Osetrov, “Experimental-theoretical limiting states of elastoplastic rods of various cross-section in extension,” in Problems of Mechanics. Collection of Papers to the 90th birthday of A. Yu. Ishlinskii [in Russian], pp. 115–123, Fizmatlit, Moscow, 2003.
[6] V. N. Kukudzhanov and V. Yu. Kibardin, “Numerical simulation of plastic strain localization and fracture of viscoelastic materials,” Izv. RAN. MTT [Mechanics of Solids], No. 1, pp. 109–119, 2000.
[7] D. A. Kazakov, D. A.‘Kapustin, and Yu. G. Korotkikh, Modeling of Deformation and Fracture Processes for Materials and Structures [in Russian], Izd-vo Nizhegorod. Un-ta, Nizhnii Novgorod, 1999.
[8] N. G. Burago and V. N. Kukudzhanov, Numerical Solution of Continual Fracture Problems, Preprint No. 746 [in Russian], In-t Problem Mekhaniki RAN, Moscow, 2004.
[9] V. D. Klyushnikov, Stability of Elastoplastic Systems [in Russian], Nauka, Moscow, 1980.
[10] J. Rice, “The localization of plastic deformation,” in Theoretical and Applied Mechanics, pp. 207–220, North-Holland, 1997.
[11] E. C. Aifantis, “The physics of plastic deformation,” Int. J. Plasticity, Vol. 3, pp. 211–247, 1987.
[12] E. I. Ryzhak, “A case of indispencible localized instability in elastic-plastic solid,” Int. J. Solids Struct., Vol. 36, pp. 4669–4691, 1999.
[13] V. I. Kondaurov and N. V. Kutlyarova, “Damage and rheological instability of initially porous materials,” Izv. RAN. MTT [Mechanics of Solids], No. 4, pp. 99–109, 2000.
[14] L. M. Kachanov, Fundamentals of Plasticity [in Russian], Nauka, Moscow, 1969.
[15] D. D. Ivleev and G. I. Bykovtsev, Theory of a Hardening Plastic Body [in Russian], Nauka, Fizmatlit, Moscow, 1971.
[16] N. Aravas, “On the Numerical Integration of a Class of Pressure-Dependent Plasticity Models,” Intern. J. Numerical Methods in Engin., Vol. 24, pp. 1395-1416, 1987.

Moscow